March 1998

MATERIALS LETTERS

ELSEVIER

Materials Letters 34 (1998) 128–132

Thermal shock behavior of ZrO_2:MgO solid electrolytes

R. Muccillo [a,*], E.N.S. Muccillo [a], N.H. Saito [b]

[a] *Instituto de Pesquisas Energéticas e Nucleares, Comissão Nacional de Energia Nuclear, C.P. 11049 - Pinheiros, 05422-970 S. Paulo, S.P., Brazil*

[b] *Instituto de Pesquisas Tecnológicas do Estado de S. Paulo, Cidade Universitária, Butantã, 05508-901 S. Paulo, S.P., Brazil*

Received 8 May 1997; accepted 18 May 1997

Abstract

Thermal shock studies have been undertaken in MgO-stabilized ZrO_2 solid electrolytes prepared from powders obtained by the citrate technique. Impedance spectroscopy and X-ray diffraction analyses have been carried out in sintered pellets before and after thermal shock at 1600°C to study phase changes. Scanning electron microscopy observations have also been performed. Thermal shock leads to a large increase in the cubic(tetragonal)-to-monoclinic phase ratio with a corresponding modification in the bulk conductivity value of the zirconia–magnesia solid electrolytes. © 1998 Elsevier Science B.V.

PACS: 81.05.Je; 81.30.-t; 84.60.Dn

Keywords: Solid electrolytes; $ZrO_2 \cdot MgO$; Oxygen sensor; Zirconia; Thermal shock; Impedance spectroscopy; Microstructure; Phase change

1. Introduction

Zirconia–magnesia ceramic solid electrolytes have been widely used as electrochemical transducers in disposable sensing devices for monitoring oxygen dissolved in molten steels [1]. Besides the electrical requirements, namely, high oxygen-ion transference number and conductivity, some of the structural requirements for these ceramics are high density to avoid molecular gas permeation, and high up-thermal shock resistance for supporting, at least during the necessary time for processing the emf signal, the sudden introduction into molten steels at temperatures usually higher than 1500°C. In the past, several results were published on thermal shock resistance of Mg-PSZ ceramics to explain the relationships between their enhanced fracture toughness and strength levels, and the microstructure features of these ceramics for structural applications [2–4]. In a previous work an experimental procedure based on the citrate technique was followed to obtain reactive zirconia–magnesia ceramic powders [5]. With these powders, solid electrolyte pellets with densities higher than 92% of the theoretical density, considered the limit for oxygen gas permeation, were obtained to be used as electrochemical transducers in sensors for measuring oxygen activity in molten steels. Here a study is described on electrical and overall microstructural changes occurring in these pellets after thermal shock experiments at 1600°C, simulating the insertion of the oxygen sensor into molten steel (up-thermal shock), and also it being withdrawn from the furnace (down-thermal shock). Two types of solid elec-

* Corresponding author. Fax: +55-118169370.

PII S0167-577X(97)00152-3

trolytes are examined: partially-stabilized (PSZ) and fully-stabilized (FSZ) zirconia–magnesia.

2. Experimental

ZrO_2 with 8.0 and 15.0 mol% MgO (nominal compositions) powders have been obtained by the citrate technique. Details of the starting materials and the experimental sequence for the preparation of the powders have already been described [5]. The powders, cold-pressed to pellets uniaxially at 100 MPa and isostatically at 184 MPa, were sintered in a gas furnace at 1600°C/3 h (200°/h up to 1200°C and 140°/h from that temperature to 1600°C) to reach densities higher than 95% of the theoretical density. Thermal shock experiments have been performed in the following way: the pellets are dropped into an alumina crucible placed inside a gas furnace previously heated up to 1600°C (up-thermal shock); after 10 min at that temperature, controlled by an optical pyrometer, the alumina crucible is removed from the furnace and the pellet is allowed to fall inside another alumina crucible kept at room temperature (down-thermal shock). The magnesium content in the ZrO_2 pellets has been determined by thermal neutron activation analysis, following a standard procedure for specimen irradiation in a swimming pool nuclear reactor: 100.0 mg of the specimen together with 2.00 mg of pure MgO standard are exposed to thermal neutrons (2.67×10^{11} n cm^{-2} s^{-1} flux) for 6 min; the ^{27}Mg photopeaks (844 keV, 9.45 min half-life) are stored, for further calculations, in a computer-controlled EG and ORTEC analyzer connected to a hyperpure Ge detector. Apparent densities have been determined by the Archimedes method (immersion in distilled water). Phase identification of sintered pellets has been done by X-ray diffraction using Rigaku Geigerflex PW3710 and X'PERT PMD Philips diffractometers. Ceramic powder morphology and grain morphology of fractured pellet surfaces have been observed in JXA 6400 JEOL and XL30 Philips scanning electron microscopes, respectively. Impedance spectroscopy measurements were carried out in the 5 Hz–13 MHz frequency range with a Hewlett Packard 4192A LF impedance analyzer connected via HPIB to an HP 900 controller, in the 300–650°C temperature range. Either sputtered Pt or Ag paste cured at 550°C were used as electrodes without any difference in the impedance spectroscopy diagrams.

3. Results and discussion

Table 1 shows results on the determination of Mg-content by thermal neutron activation analysis and the apparent densities of the zirconia–magnesia specimens with 8 mol% and 15 mol% nominal compositions. The values determined by neutron activation analysis are smaller to the added values and taken as the actual magnesia content in these specimens due to the accuracy of the method. The studied specimens are hereafter referred either as PSZ or 7.5 mol% MgO, and FSZ or 11.9 mol% MgO. For the determination of the percent value of the theoretical densities, the following values have been assumed as the theoretical densities: 5.83 g cm^{-3} for the PSZ [6] and 5.80 g cm^{-3} for the FSZ [7]. The relative monoclinic phase content V_m is also shown. Their evaluation has been done using the Porter and Heuer equation: $V_m = 1.609I_m\,[11\text{-}1]/(1.609I_m\,[11\text{-}1] + I_c\,[111])$, I_m and I_c being the peak intensities of the 100% monoclinic and cubic diffraction lines, respectively [8]. The thermal shock experiment led to an enhancement of the amount of the room temperature

Table 1
Values of nominal and determined MgO content, apparent density and monoclinic phase content (V_m) in ZrO_2:MgO sintered ceramic pellets

Nominal MgO-content (mol%)	Determined MgO-content (mol%)	Hydrostatic density		V_m (%) before thermal shock	V_m (%) after thermal shock
		g/cm^3	%TD		
8.0	7.5	5.64	96.7	75	20
15.0	11.9	5.49	94.7	28	0

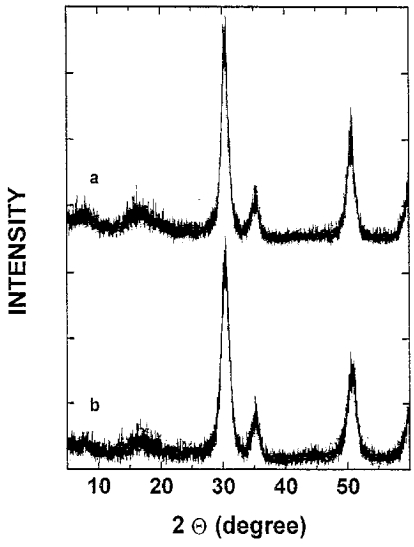

Fig. 1. X-ray diffraction patterns of ZrO_2:7.5 mol% MgO (a) and ZrO_2:11.9 mol% MgO (b) powders prepared by the citrate technique.

metastable cubic phase at the expenses of the monoclinic phase content.

Fig. 1 shows X-ray diffraction spectra of ZrO_2:7.5 mol% MgO (1a) and ZrO_2:11.9 mol% MgO (1b) powders obtained by the citrate technique and calcined at 800°C [5].

These results show that both powders are single phase tetragonal with the main diffraction lines at $2\theta = 30.2°$ (1,1,1; 100%), 49.8° (2,0,2; 65%) and 35.3° (0,0,2; 25%); the first three figures are the Miller index and the last the relative diffraction line intensity.

Typical microstructure features of the as-calcined ZrO_2:7.5 mol% MgO powders are shown in Fig. 2. Small aggregates are seen along with agglomerates larger than 20 μm. Those aggregates/agglomerates are relatively soft once high apparent densities (determined by the hydrostatic technique) have been reached after powder compacting and sintering. Fully-stabilized powders present similar microstructure features.

Fig. 3 shows X-ray diffraction spectra of the ZrO_2:7.5 mol% MgO and ZrO_2:11.9 mol% MgO sintered pellets before (a and c) and after (b and d) thermal shock from 1600°C to room temperature. The powders have been pressed (uniaxially at 100 MPa and isostatically at 184 MPa), and sintered at 1600°C for 3 h.

Fig. 3 shows the main evidences of structural phase changes after submitting sintered zirconia–magnesia pellets to thermal shock at 1600°C. An increase in the (cubic + tetragonal)-to-monoclinic phase ratio is clearly shown, as expected due to the frozen-in at room temperature of the phases that are stable at 1600°C. For the Mg-fully stabilized zirconia (Fig. 3c and d), on the other hand, no monoclinic diffraction lines are detected after thermal shock from 1600°C to room temperature, i.e., the specimen is in the cubic phase. The values determined for the monoclinic phase content are shown in Table 1.

In Fig. 4 typical micrographs of fractured surfaces after thermal shock are shown for ZrO_2:7.5 mol% MgO (4a) and ZrO_2:11.9 mol% MgO (4b) pellets. Both specimens have kept their physical integrity after the up-to-1600°C and down-to-RT thermal shock cycle. The microstructure features of Fig. 4a are typical of partially stabilized zirconias: intergranular fracture mode and smaller grains are observed. On the other hand, coarse grains of approximately 20 μm in diameter and intragranular porosity are the main microstructure characteristics observed in Fig. 4b, usually found in fully stabilized zirconia-based ceramics. Both specimens presented some surface cracks, but no internal cracks and/or microcracks are seen.

Impedance spectroscopy measurements have been carried out at 750 K in ZrO_2:MgO specimens before and after thermal shock. In Fig. 5, impedance dia-

Fig. 2. Scanning electron microscopy micrograph of ZrO_2:7.5 mol% MgO powders prepared by the citrate technique.

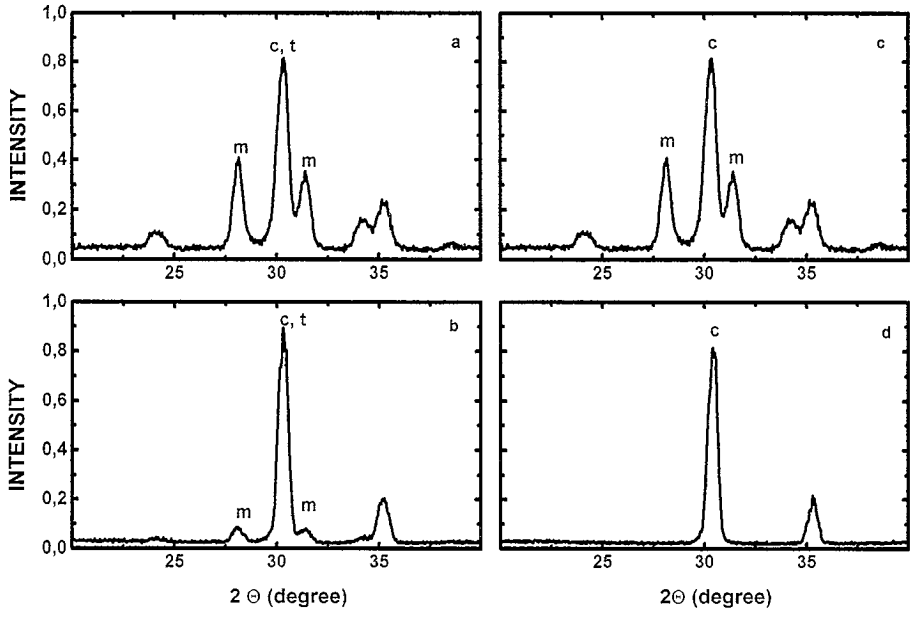

Fig. 3. X-ray diffraction patterns of ZrO_2:7.5 mol% MgO pellets: (a) before and (b) after thermal shock from 1600°C to RT. (c) and (d) refer to ZrO_2:11.9 mol% MgO pellets.

grams of ZrO_2:7.5 mol% MgO (Fig. a) and ZrO_2:11.9 mol% MgO (Fig. b) specimens before and after thermal shock are shown. Before the thermal shock the PSZ specimen shows an impedance diagram with overlapping of the contributions from intergrain and intragrain components, whereas after thermal shock the semicircle due to the intragrain component is somehow better resolved. This is an evidence that the less resistive phases (cubic and/or tetragonal) content has increased at the expenses of the blocking phase (monoclinic), in agreement with the X-ray diffraction results. The FSZ specimen, on the other hand, shows before thermal shock a more resolved diagram because it has already a lower monoclinic phase content (cf. Table 1). After thermal shock, the impedance diagram is typical of fully stabilized zirconias, presenting both semicircles due to inter- and intragrain resistivities [9–11]. Moreover, after thermal shock the intragrain resistivity is higher than before suggesting that the tetragonal phase is less resistive than the cubic one (there is no tetragonal phase after thermal shock). One should also consider that the cubic phase has extensive intragranular porosity, which could lead to a larger intragrain semicircle [12]. Another feature of Fig. 5 is that the intragrain resistivity of the PSZ specimen is much smaller than that of the FSZ, becoming evident that thermal treatments that avoid monoclinic phase formation help to obtain high conductivity PSZ specimens. A detailed analysis of impedance diagrams of the 11.9 mol%-stabilized ZrO_2 at different temperatures allowed for the determination of the activation energy of the ionic conduction process for the inter- and the intragrain conductivity, 1.4 eV, and also of the dielectric constant, 46, in agreement with previous results [9]. The extrapolated value of the ionic conductivity at 1000°C has also been determined: 0.135 S cm^{-1}, of the same order of magnitude of a recent reported value, 0.072 S cm^{-1} [13].

The impedance diagrams of the specimens measured before thermal shock experiments are typical of partially stabilized ZrO_2:MgO solid electrolytes: a not easy to separate overlapped bulk, monoclinic (blocking) phase, grain boundary and electrode polarization contributions to the electrical resistivity [9–11]. After thermal shock, a decrease in the electrical resistivity is clearly seen, due to the enhancement in electrical conductivity caused by the increase in the cubic-to-monoclinic structural phase ratio in the ceramic specimens. It is already known

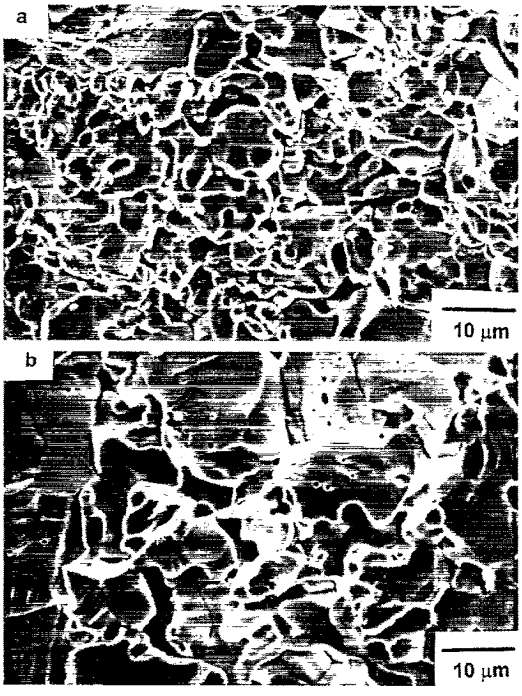

Fig. 4. SEM micrographs of ZrO_2:7.5 mol% MgO (a) and ZrO_2:11.9 mol% MgO (b) fractured pellets after thermal shock from 1600°C to RT.

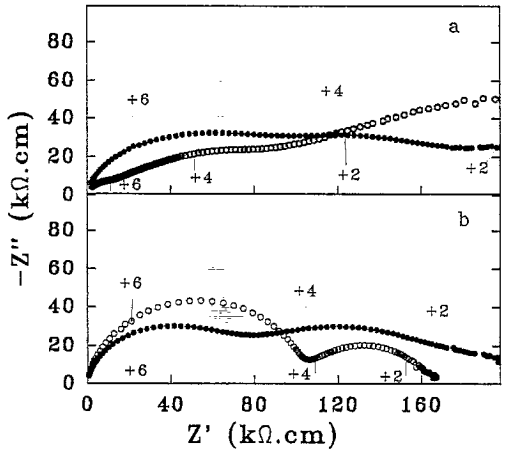

Fig. 5. Impedance diagrams at 750 K of (a) ZrO_2:7.5 mol% MgO and (b) ZrO_2:11.9 mol% MgO pellets before (filled circles) and after (hollow circles) thermal shock from 1600°C to RT.

that the ionic conductivity of cubic stabilized ZrO_2 ceramics is larger than that of monoclinic ZrO_2 [13].

4. Conclusions

ZrO_2:MgO solid electrolytes prepared from powders processed by the citrate technique have high resistance to up- and down-thermal shock at 1600°C. The thermal shock behavior has been followed by X-ray and impedance spectroscopy measurements before and after thermal shock. The increase in electrical conductivity after thermal shock is in agreement with the increase in the cubic-to-monoclinic phase ratio detected by X-ray measurements.

Acknowledgements

We acknowledge Dr. A.M.G. Figueiredo for neutron activation analyses and FAPESP (contract 92-2962/6) for financial support.

References

[1] E.C. Subbarao (Ed.), Solid Electrolytes and their Applications, Plenum Press, New York and London, 1980.
[2] R.H.J. Hanninck, R.C. Garvie, J. Mater. Sci. 17 (1982) 2637–2643.
[3] A.H. Heuer, L.H. Schoenlein, J. Mater. Sci. 20 (1985) 3421–3427.
[4] P.F. Becher, M.K. Ferber, J. Mater. Sci. 22 (1987) 973–980.
[5] R. Muccillo, N.H. Saito, E.N.S. Muccillo, Mater. Lett. 25 (1995) 165–169.
[6] R. Stevens, Magnesium Elektron Publ. N. 113 (1986).
[7] I. Abraham, G. Gritzner, J. Eur. Ceram. Soc. 16 (1996) 71–77.
[8] D.L. Porter, A.H. Heuer, J. Am. Ceram. Soc. 62 (1979) 298.
[9] E.N.S. Muccillo, M. Kleitz, J. Eur. Ceram. Soc. 15 (1995) 51–55.
[10] E.N.S. Muccillo, M. Kleitz, J. Eur. Ceram. Soc. 16 (1996) 453–465.
[11] E.N.S. Muccillo, Ph.D. Thesis (in Portugese), IPEN-USP, S. Paulo, Brazil, 1993.
[12] J.R. McDonald (Ed.), Impedance Spectroscopy – Emphasizing Solid Materials and Systems, Wiley Interscience, New York, 1987.
[13] E. Butler, N. Bonanos, Mater. Sci. Eng. 71 (1985) 49.